Pure Appl. Chem., Vol. 80, No. 8, pp. 1873–1882, 2008.
doi:10.1351/pac200880081873

Artificial tongues and leaves*

Natalie Banerji, Rajesh Bhosale, Guillaume Bollot, Sara M. Butterfield, Alexandre Fürstenberg, Virginie Gorteau, Shinya Hagihara, Andreas Hennig, Santanu Maity, Jiri Mareda, Stefan Matile‡, Federico Mora, Alejandro Perez-Velasco, Velayutham Ravikumar, Ravuri S. K. Kishore, Naomi Sakai, Duy-Hien Tran, and Eric Vauthey

Departments of Organic and Physical Chemistry, University of Geneva, Geneva, Switzerland

Abstract: The objective with synthetic multifunctional nanoarchitecture is to create large suprastructures with interesting functions. For this purpose, lipid bilayer membranes or conducting surfaces have been used as platforms and rigid-rod molecules as shape-persistent scaffolds. Examples for functions obtained by this approach include pores that can act as multicomponent sensors in complex matrices or rigid-rod π-stack architecture for artificial photosynthesis and photovoltaics.

Keywords: nanoarchitecture; sensors; photovoltaics; photosynthesis; lipid bilayer; scaffolds.

The objective with synthetic multifunctional nanoarchitecture is to create large suprastructures with interesting functions [1,2]. To address this challenge, we often begin with lipid bilayer membranes or, more recently, conducting surfaces as platforms. To direct, control, and stabilize advanced functional architecture, rigid-rod molecules [3–10] have been introduced as shape-persistent scaffolds. Somehow the antithesis to foldamers [11,12], these simple sturdy rods are attractive scaffolds, bypassing all folding problems because they do not fold. Unknown in biology, rigid-rod molecules are much appreciated in the materials sciences [3]. Prominent members of this family of oligomeric molecules include oligoacetylene **1**, *p*-oligophenyls **2** [4,5] and their formal mixture, i.e., *p*-oligophenyleneethynylene (OPE) rods **3** [6,7] (Fig. 1). Whereas the benzene rings in *p*-oligophenyls **2** and OPEs **3** can rotate more or less freely, oligonaphthalenes **4** cannot. This produces an exceptionally complex axial stereochemistry [8]. Rigid oligonaphthalenediimide (O-NDI) rods **5** [9] and oligoperylenediimides (O-PDI) rods **6** [10] are of interest because they are colorizable, π-acidic n-semiconductors. Oligoporphyrins are extensively studied because of their optoelectric properties, the nonplanar rod **7** has been elongated up to l = 1060 Å of the monodisperse 128-mer [11].

From this rich collection of rigid-rod molecules, we originally selected *p*-oligophenyls **2** as model rods [1,2,14]. *p*-Oligophenyls are not only straightforward to synthesize and derivatize but also nonplanar and fluorescent, and can exhibit a dynamic axial chirality. The torsion angles between neighboring phenyls of the *p*-oligophenyl scaffold provide the directionality that is needed to control advanced supramolecular architecture. Dynamic chirality and fluorescence are of use for structural studies in

*Paper based on a presentation at CHEM-BIO-TECH-2007, a joint meeting of the IUPAC 1st Symposium on Chemical Biotechnology (ISCB-1) and the 8th Symposium on Bioorganic Chemistry (ISBOC-8), 8–11 August 2007, Turin, Italy. Other presentations are published in this issue, pp. 1773–1882.

‡Corresponding author: E-mail: stefan.matile@chiorg.unige.ch

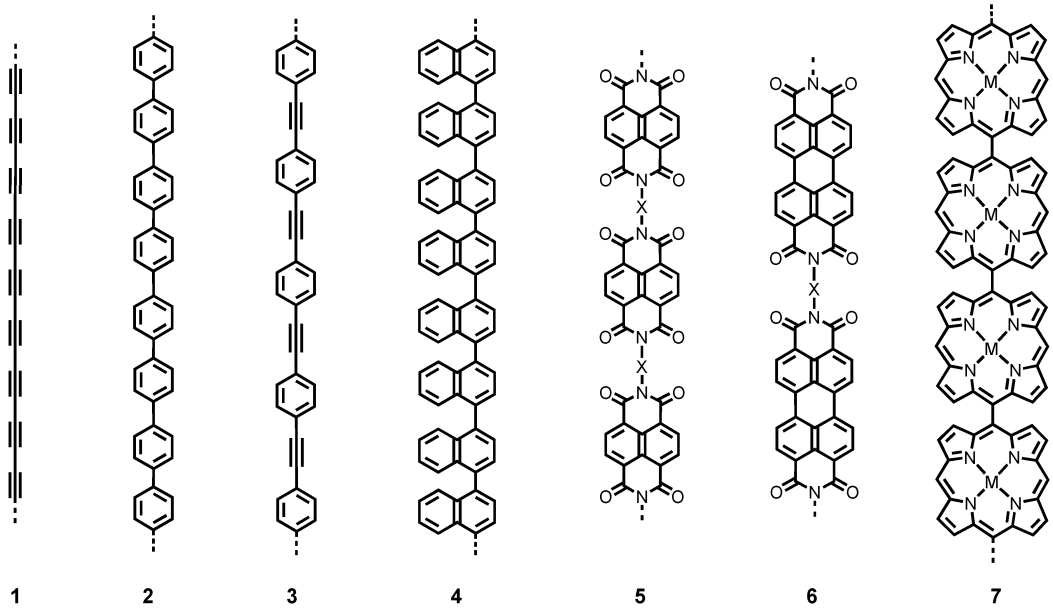

Fig. 1 Some rigid-rod molecules.

more complex systems under conditions that are relevant for significant function. Usually, these are nanomolar to low micromolar rod concentrations in lipid bilayers. Only recently, we started to expand into O-NDIs **5** [15,16], O-PDIs **6**, and OPEs **3**, mainly for applications toward photosynthesis and photovoltaics.

Functional rigid-rod nanoarchitectures that have been synthesized over the years include proton wires **8**, anion-π slides **9**, push-pull rods **10**, artificial β-barrels **11**, and helical π-stacks **12** (Fig. 2). In rod **8**, a hydrogen-bonded chain was built along the transmembrane scaffold to selectively transport protons across lipid bilayer membranes [17]. In the envisioned hop-turn proton hopping mechanism, one proton binds to one end of the hydrogen-bonded chain, and the proton at the other end at the other side of the membrane is released. This proton hopping mechanism is thought to be essential in bioenergetics and may be of use in fuel cells.

The anion-π slide **9** is a representative member of a recently introduced system [15,16]. It complements early cation-π slides, where cation-π interactions along ligand-assembled *p*-octiphenyl scaffolds are used to transport potassium cations across bilayer membranes [18]. Compared to the straightforward interactions of cations with conventional π-basic aromatic rings, the creation of functional systems that operate on anion-π interactions is much more demanding because it requires rigid-rod scaffolds that contain π-acidic aromatic rings. The positive quadrupole moment Q_{zz} = +19.4 B of NDIs, well beyond the classical hexafluorobenzene (Q_{zz} = +8.9 B), identified (O-NDI) rods **9** as ideal for this purpose [15,16]. The found cooperative selectivity for small anions with high dehydration penalty revealed strong binding and multi-ion hopping along transmembrane bundles of the π-acidic O-NDI rods **9** without significant contributions from size exclusion.

Push-pull rods such as **10** were introduced to explore the role of dipole-potential interactions for voltage gating in a broad sense [19,20]. In these shape-persistent α-helix mimics [21], a π-donor D at one and a π-acceptor A at the other end introduces a macrodipole along the rod axis. Different from the macrodipole of α-helices, this rigid-rod dipole is not subject to conformational changes but can be readily turned off without global structural changes. Moreover, this shape-persistent macrodipole is intrinsically fluorescent. To complement structural studies by fluorescence depth quenching with information on function, push-pull rod **10** carries ionophoric crown ethers along the rigid-rod scaffold. This

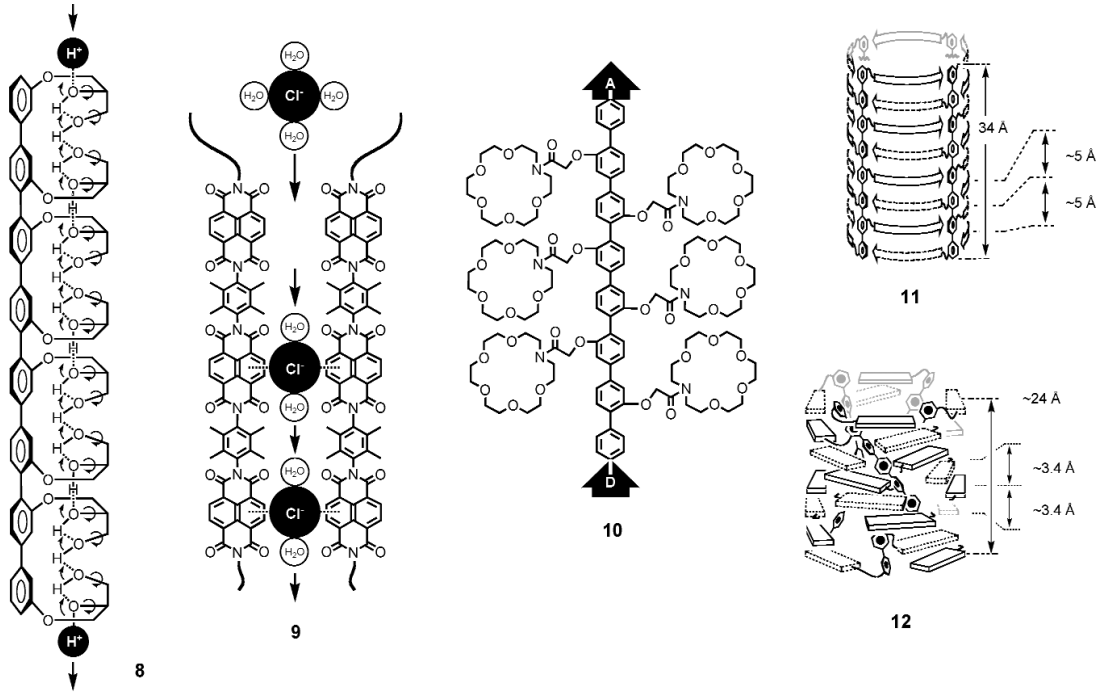

Fig. 2 Functional rigid-rod architectures synthesized over the last decade include, from left to right, proton wires, anion-π slides, push-pull rods, artificial β-barrels, and helical π-stacks.

push-pull approach provided a variety of voltage-gated ion channels including **10** [19,20] or push-pull β-barrels [22,23]. Moreover, experimental evidence in support of the importance of membrane polarization for the mechanism of action of natural antibiotics could be secured, also on the structural level [20].

Rigid-rod β-barrels with the general structure **11** are barrel-stave supramolecules composed of rigid-rod staves and β-sheets hoops [1,2]. Rigid-rod β-barrels with *p*-oligophenyl staves exhibit perfect hoop-stave matching. The repeat distance of 5.0 Å adds up to eight-stranded β-sheets with the length that matches that of a *p*-octiphenyl rod. Replacement of the β-sheets in rigid-rod β-barrels **11** by π-stacks with a repeat distance of ~3.4 Å introduces a hoop-stave mismatch. To minimize this mismatch and maximize face-to-face π–π interactions, the barrel-stave architecture twists into π-helices **12**. Easily visualizable with a hyperboloid, this barrel-helix transition contracts the internal space of the barrel-stave architecture (under the condition that the rods are rigid and sticky, i.e., can neither bend nor translocate along each other). The resulting rigid-rod π-helices **12** can transport electrons but not molecules across lipid bilayers. Simply speaking, barrel-stave architecture **11** is thus ideal to create pores for use as multianalyte sensors, whereas π-helices **12** are ideal for photosynthesis. Recent results on both systems are described in more detail in the following.

Synthetic access to rigid-rod β-barrel architecture **11** was essential to build pores for multicomponent sensing in complex matrices (Figs. 3 and 4) [24,25]. The possibility of precisely positioning amino acid residues on β-sheets allows us to variably functionalize both inner and outer surfaces of rigid-rod β-barrels in a rational manner (Fig. 4). Hydrophobic outer and hydrophilic inner surfaces give pores in lipid bilayer membranes. The addition of binding sites at inner or outer pore surfaces introduces the responsiveness that is needed for sensing. For this purpose, the applicability of synthetic multifunctional pores as optical transducers of reactions is ideal [26]. With sensitivity toward changes in charge or bulk, optical transduction with synthetic pores is compatible with a broad range of reac-

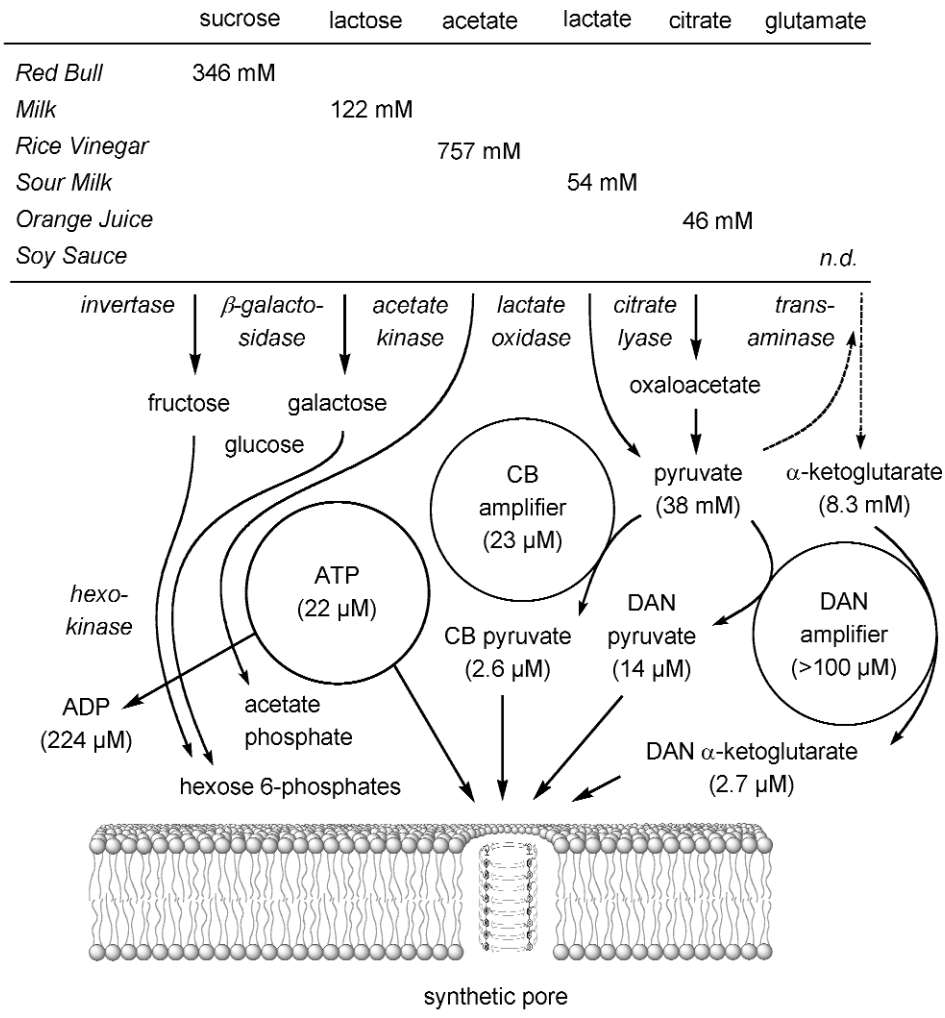

Fig. 3 An artificial tongue to illustrate multicomponent sensing in complex matrices with synthetic pores and reactive amplifiers. The shown analyte concentrations are values measured in samples from the supermarket after signal generation with enzymes and cosubstrates (e.g., ATP), eventual signal amplification with CB or DAN hydrazides (Fig. 4), and signal transduction with synthetic pores. Concentrations in parenthesis are IC_{50} values for blockage and refer to pore **11A** except for DAN data referring to pore **11B**; n.d., not determined. Individual analyses were done separately and not in the same vial.

tions [27]. In practice, their general use is similar to chromatographic methods such as high-performance liquid chromatography (HPLC) or thin layer chromatography (TLC) with regard to both scope and simplicity. The combination with enzymes as specific signal generators is particularly attractive (Figs. 3 and 4) [26]. The broad compatibility of synthetic pores with many reactions assures detectability of the activity of many different enzymes [27]. This adaptability assures applicability of pore transducers in various fields, including drug discovery (enzyme inhibitor screening) and diagnostics.

One central challenge concerning the practical application of sensors in diagnostics is the sensing of multiple analytes in complex matrices from the supermarket or the hospital [28–31]. To address this challenge with synthetic pores, the creation of artificial tongues was an obvious choice because also on our own tongues, the sensation of taste is mediated by pores that respond to chemical stimulation [32].

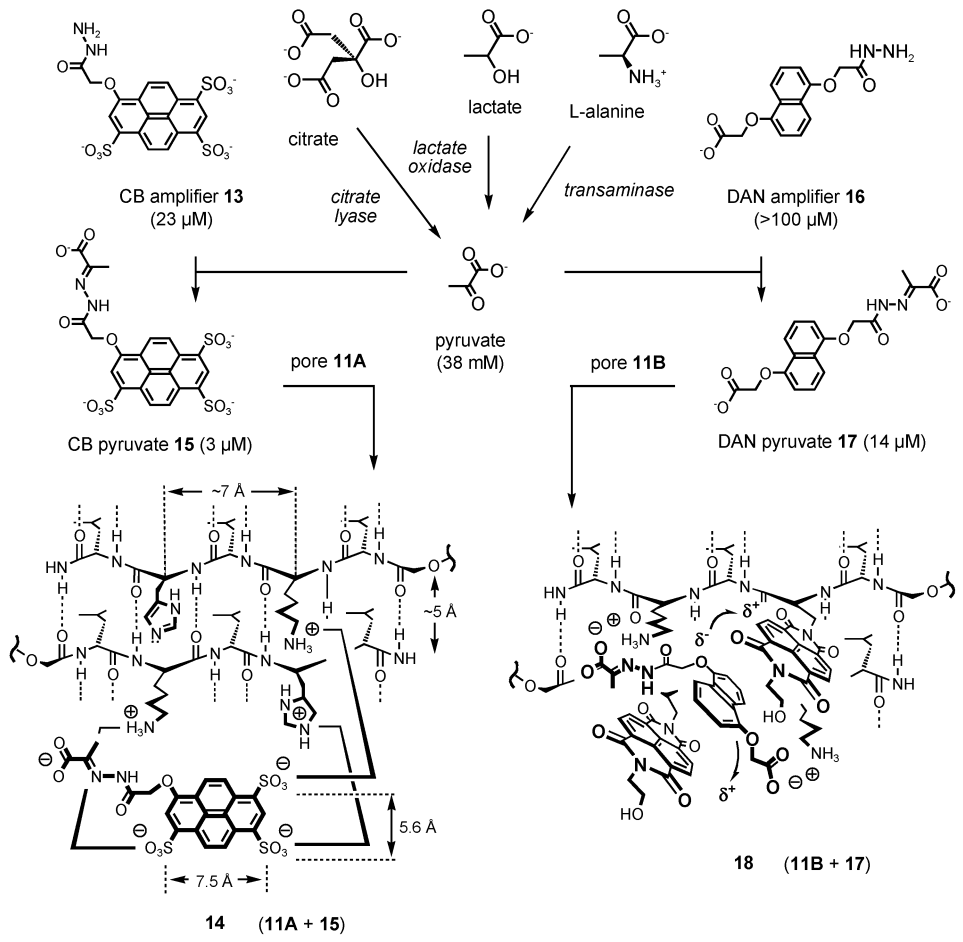

Fig. 4 Representative sensing scheme for the artificial tongue outlined in Fig. 3. Adaptable signal generation for citrate, lactate, and alanine is followed by reactive amplification for recognition by multipoint ion pairing within pore **11A** (sequence LKLHL) and π–clamping within pore **11B** (sequence Lπ_ALKL).

To elaborate on synthetic pores as artificial tongues, sugar sensing was envisioned first [33]. It was accomplished with synthetic pore **11A** (i.e., rigid-rod β-barrel with peptide sequence LKLHL). The diagonal positioning lysines and histidines at the inner surface makes these pores more responsive to blockage by adenosine 5'-triphosphate (ATP) than by adenosine 5'-diphosphate (ADP). To use this precious ATP/ADP discrimination for sugar sensing, soft drinks such as Coca Cola or Red Bull were incubated first with invertase as specific signal generator. The obtained glucose and fructose were then treated with hexokinase and ATP. The consumption of the ATP blocker during phosphorylation was optically transduced as fluorogenic pore opening (Fig. 3).

The sensing of lactose in milk was targeted next [34]. The strategy developed for sucrose sensing was applicable with minor changes. Replacement of invertase with β-galactosidase was all that was needed to switch the selectivity of signal generation from sucrose to lactose. Consumption of the ATP blocker during selective phosphorylation of the products with hexokinase was used for quantitative detection of lactose levels in milk serum with pore **11A**.

The sensing of the acetate in vinegar with synthetic pore **11A** was realized as well [34]. Acetate sensing was again possible following the conversion of ATP into ADP as fluorogenic pore opening. The

specific signal generator used was acetate kinase, which directly and quantitatively links ATP consumption with the concentration of acetate.

The sensing of lactate in milk was realized next to enrich the repertoire of synthetic pores as artificial tongues [34]. This topic turned out to be scientifically more demanding. Lactate oxidase was on hand as signal generator. However, synthetic pores that would recognize either the substrate lactate or the product pyruvate could neither be found nor made. To address this challenge, we introduced the concept of reactive amplification.

We define reactive amplifiers as compounds that can (a) block or open synthetic pores and (b) react spontaneously with the functional group produced or consumed during an otherwise elusive reaction. Reactive amplification conceptually related to pre- or post-column derivatization strategies in chromatography or electrophoresis. A similar covalent capture process was found last year to also occur on our own tongue to make the experience of mustard or cinnamon oil a long-lasting one [35].

With the introduction of reactive amplifiers, the problem of lactate sensing with synthetic pores was solved [34]. CB (Cascade Blue) hydrazide **13** was selected as amplifier because, on the one hand, it reacts spontaneously with aldehydes and ketones to give stable hydrazone products. On the other hand, the blockage of rigid-rod β-barrel pores by 3,6,8-pyrenetrisulfonates is very well understood (Fig. 4). Recent model studies with β-hairpin macrocycles confirmed multipoint ion pairing in complexes such as **14** as origin of this useful function [36].

For lactate sensing, amplifier **13** was applied to covalently capture the elusive pyruvate produced during signal generation with lactate oxidase [34]. CB hydrazone **15** was obtained in mildly acidic water and was stable in neutral water. This reactive amplification improved the sensitivity of pyruvate detection by pore **11A** by more than four orders of magnitude. Moreover, the small increase in bulk and charge during amplification was sufficient to avoid interference from unreacted amplifier **13**.

The sensing of the sour citrate in orange juice was addressed next [34]. Citrate sensing was an excellent example to illustrate the general applicability of the concept of reactive amplification. To switch the selectivity from lactate to citrate, citrate lyase instead of lactate oxidase was used as signal generator. In a typical procedure, orange juice was incubated first with a hydrazine-rich resin to minimize interference from aldehydes and ketones as hydrazones. Incubation with citrate lyase then gave oxaloacetate, which presumably decarboxylated spontaneously to pyruvate. Amplification by covalent capture with CB hydrazide **13** then produced CB hydrazide **14** for the blockage of pore **11A**.

To complement the realized examples for the sensing of sweet and sour components in samples from the supermarket, umami sensing in soy sauce was considered [34]. Signal generation with glutamate oxidase and amplification of α-ketoglutarate with CB hydrazide **13** was an obvious option. Signal generation with aminotransferases was an attractive alternative because the challenge of selective signal amplification could be addressed. Aminotransferases catalyze the transfer of the amine of glutamate to the cosubstrate pyruvate, yielding α-ketoglutarate and alanine. With hydrazide amplifiers, the specific question therefore was whether or not α-ketoglutarate could be amplified without interference from pyruvate. Selective amplification with CB hydrazide **11** failed. So far, the best selectivity was obtained with dialkoxynaphthalene (DAN) amplifier **16**. This π-basic amplifier is recognized within the synthetic pore **11B** [37,38]. In this pore, artificial amino acids with π-acidic NDI side chains are positioned at the inner pore surface (Fig. 4). Two NDIs within pore **11B** are placed in ideal distance to act like molecular clamps or tweezers and catch amplifier-analyte conjugates such as **17** and form donor–acceptor complexes such as **18**. The validity of the concept of π-clamps or tweezers has been confirmed for many different motifs including synthetic β-hairpins [39].

Photosystem **12** was obtained by replacement of the β-sheets in barrel-stave supramolecules **11** with π-stacks (Figs. 2 and 5) [40–42]. The mismatch between π-stack repeat and *p*-octiphenyl length causes the barrel-stave supramolecule to twist and close. The resulting π-helix is impermeable for molecules but can transport electrons through the π-stack. Rigid-rod π-stack architecture appeared perfect for the creation of photosynthetic activity.

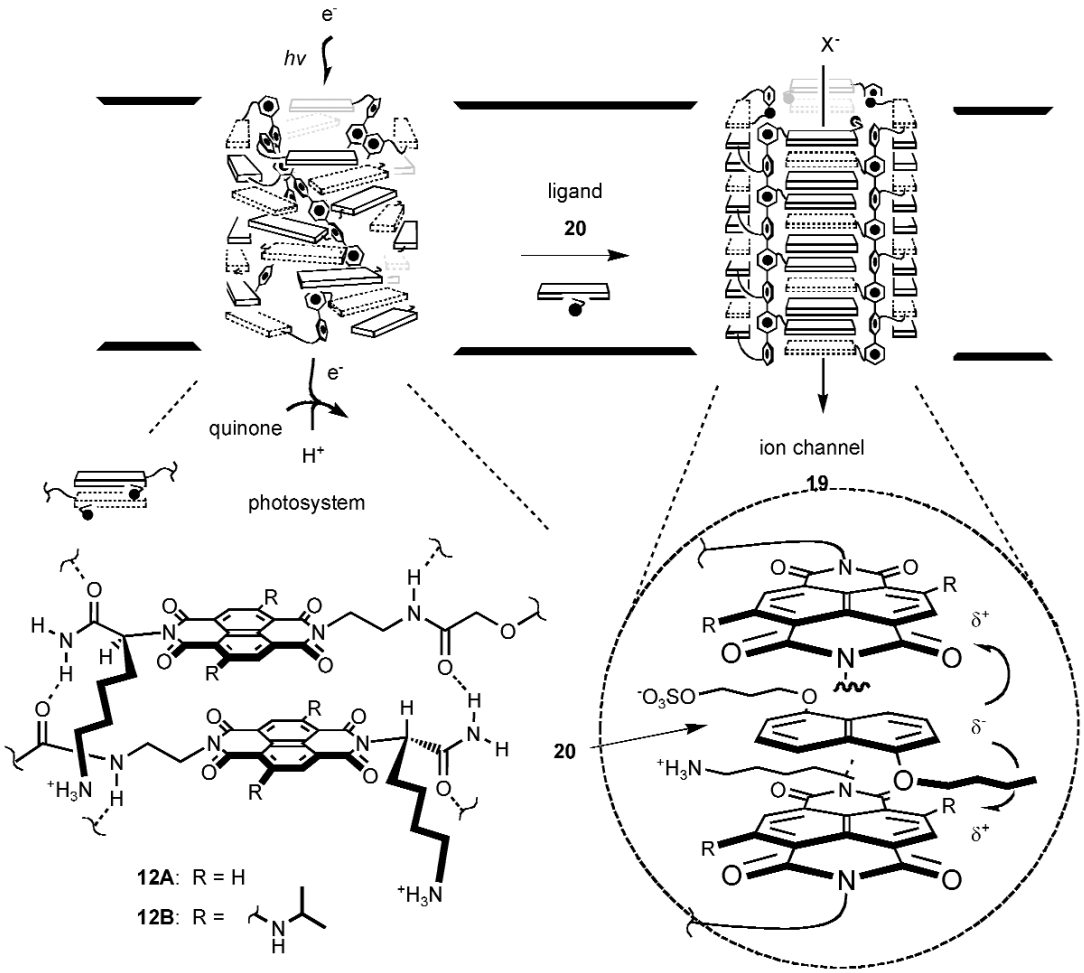

Fig. 5 Rigid-rod π-stack helices **12** with photosynthetic activity that can untwist into barrel-stave architecture **19** with ion channel activity in response to the intercalation of ligands **20**.

NDIs were selected to create rigid-rod π-stack architecture **12**. This choice was made because the planarity and π-acidity of NDIs is ideal for face-to-face π-stacking. Moreover, NDI π-stacks are among the few air-stable n-semiconductors. Most importantly, photo- and electrochemical properties of NDIs can be easily varied without global structural change [43,44]. The introduction of two alkylamines in the core of the NDI converts the colorless substrate into a blue, red-fluorescent chromophore. Replacement of one amine by an ether, that is one nitrogen by an oxygen, produces a red chromophore with orange fluorescence. Replacement of the second nitrogen by another oxygen gives a yellow, green-fluorescent chromophore. With increasingly powerful π-donors in the core, this decrease in bandgap coincides with decreasing π-acidity as well as decreasing reduction and oxidation potentials.

To create multifunctional rigid-rod π-stack architecture, *p*-octiphenyls with eight cationic NDIs were prepared. Amides were added at both sides of the NDI to orient the π-stacks with H-bonded chains [45,46]. Denaturation-corrected Hill analysis demonstrated self-assembly into tetrameric architecture as expected for π-helix **12** [42]. The appearance of the hypsochromic maximum next to the low-energy NDI transition demonstrated face-to-face π-stacking [40]. The circular dichroism (CD) spectrum revealed *M*-helicity of the exciton-coupled NDI chromophores.

In nanoarchitecture **12B**, the optoelectrical properties of the blue NDI suggested that the stacked chromophore array could not only serve as chromophore but also as electron acceptor and electron donor. This implied that transient photoinduced charge separation could occur with minimal loss of photonic energy. Time-resolved fluorescence decay confirmed the occurrence of ultrafast (<2 ps) and quantitative charge separation [40]. The $NDI^{-\bullet}$ radical anion could be directly detected by transient absorption spectroscopy. Decay kinetics of this $NDI^{-\bullet}$ radical anion revealed that photoinduced charge separation in photosystem **12B** lasts relatively long for a system without donor–acceptor dyads (61 ps).

Photosynthetic activity of rigid-rod π-helix **12B** was studied in lipid bilayer vesicles [40]. These vesicles were loaded with quinones as electron acceptors, and ethylenediaminetetraacetic acid (EDTA) was added externally as electron donor. Their redox potentials are appropriate to oxidize the photosystem **12B** on the one side and fill the hole on the other side of the bilayer membrane. This photoredox process is thermodynamically unfavorable and thus converts photonic into chemical energy. Proton consumption during intravesicular quinone reduction could be readily measured by fluorometric detection of changes in intravesicular pH. The photosynthetic activity was characterized by a Hill coefficient of four. This revealed the occurrence of supramolecular function, i.e., that tetrameric rigid-rod π-helix **12B** accounts for photosynthetic activity. Controls confirmed that monomeric or disorganized NDI dimers have no photosynthetic activity.

Photosystem **12B** was designed to open up into ion channels **19** in response to chemical stimulation (Fig. 5) [40,45,46]. Electron-rich DANs **20** were used as ligands to intercalate into π-helix **12**. Ligand intercalation was expected to reduce the hoop-stave mismatch. This ligand gating thus causes the opening up into the barrel-stave supramolecule **19** with a channel in the center of the molecule. Central in chemistry and biology of oligonucleotides, intercalation into π-stack nanoarchitecture is rare in biomembrane function, not to speak of synthetic ion channels and pores [47–56]. Functional and structural studies revealed that the helix-barrel transition from photosystem **12B** to ion channel **19** is highly cooperative, sensitive, and selective with regard to ligand and channel structure. Ion channels **19** are small, anion-selective, ohmic, and remarkably homogenous considering the complexity of the architecture [46].

In summary, it is possible to synthesize supramolecular architectures that can function as ion channels, pores, or photosystems. Rigid-rod molecules emerge as privileged scaffolds for this purpose. As far as perspectives are concerned, multicomponent sensing with pores calls for development and applications in the broadest sense (analytes, enzymes, amplifiers, pores [57], modes of detection). With regard to photosystems, it will be important to move on from bilayer membranes to conducting surfaces and explore if and how rigid-rod π-stack architecture can contribute to the generation of currents with light.

ACKNOWLEDGMENTS

We warmly thank all past coworkers and all past and present collaborators for much appreciated contributions, and the University of Geneva and the Swiss NSF for financial support.

REFERENCES

1. N. Sakai, J. Mareda, S. Matile. *Acc. Chem. Res*. **38**, 79 (2005).
2. R. Bhosale, S. Bhosale, G. Bollot, V. Gorteau, M. D. Julliard, S. Litvinchuk, J. Mareda, S. Matile, T. Miyatake, F. Mora, A. Perez-Velasco, N. Sakai, A. L. Sisson, H. Tanaka, D.-H. Tran. *Bull. Chem. Soc. Jpn*. **40**, 1044 (2007).
3. M. D. Levin, P. Kaszynski, J. Michl. *Chem. Rev.* **100**, 1863 (2000).
4. F. Cacialli, J. S. Wilson, J. J. Michels, C. Daniel, C. Silva, R. H. Friend, N. Severin, P. Samori, J. P. Rabe, M. J. O'Connell, P. N. Taylor, H. L. Anderson. *Nat. Mater.* **1**, 160 (2002).
5. W.-Y. Yang, J.-H. Ahn, Y.-S. Yoo, N.-K. Oh, M. Lee. *Nat. Mater.* **4**, 399 (2005).

6. D. Ickenroth, S. Weissmann, N. Rumpf, H. Meier. *Eur. J. Org. Chem.* 2808 (2002).
7. J. N. Clifford, T. Gu, J.-F. Nierengarten, N. Armaroli. *Photochem. Photobiol. Sci.* **5**, 1165 (2006).
8. K. Tsubaki. *Org. Biomol. Chem.* **5**, 2179 (2007).
9. L. L. Miller, B. Zinger, J. S. Schlechte. *Chem. Mater.* **11**, 2313 (1999).
10. M. J. Ahrens, L. E. Sinks, B. Rybtchinski, W. Liu, B. A. Jones, J. M. Giaimo, A. V. Gusev, A. J. Goshe, D. M. Tiede, M. R. Wasielewski. *J. Am. Chem. Soc.* **126**, 8284 (2004).
11. N. Aratani, A. Osuka, Y. H. Kim, D. H. Jeong, D. Kim. *Angew. Chem., Int. Ed.* **39**, 1458 (2000).
12. S. H. Gellman. *Acc. Chem. Res.* **31**, 173 (1998).
13. D. J. Hill, M. J. Mio, R. B. Prince, T. S. Hughes, J. S. Moore. *Chem. Rev.* **101**, 3893 (2001).
14. N. Sakai, K. C. Brennan, L. A. Weiss, S. Matile. *J. Am. Chem. Soc.* **119**, 8726 (1997).
15. V. Gorteau, G. Bollot, J. Mareda, A. Perez-Velasco, S. Matile. *J. Am. Chem. Soc.* **128**, 14788 (2006).
16. V. Gorteau, G. Bollot, J. Mareda, S. Matile. *Org. Biomol. Chem.* **5**, 3000 (2007).
17. L. A. Weiss, N. Sakai, B. Ghebremariam, C. Ni, S. Matile. *J. Am. Chem. Soc.* **119**, 12142 (1997).
18. M. M. Tedesco, B. Ghebremariam, N. Sakai, S. Matile. *Angew. Chem., Int. Ed.* **38**, 540 (1999).
19. J.-Y. Winum, S. Matile. *J. Am. Chem. Soc.* **121**, 7961 (1999).
20. N. Sakai, D. Gerard, S. Matile. *J. Am. Chem. Soc.* **123**, 2517 (2001).
21. J. M. Davis, L. K. Tsou, A. D. Hamilton. *Chem. Soc. Rev.* **36**, 326 (2007).
22. N. Sakai, S. Matile. *J. Am. Chem. Soc.* **124**, 1184 (2002).
23. N. Sakai, N. Sordé, S. Matile. *J. Am. Chem. Soc.* **125**, 7776 (2003).
24. N. Sakai, N. Majumdar, S. Matile. *J. Am. Chem. Soc.* **121**, 4294 (1999).
25. N. Sakai, S. Matile. *Chem. Commun.* **38**, 2514 (2003).
26. G. Das, P. Talukdar, S. Matile. *Science* **298**, 1600 (2002).
27. N. Sordé, G. Das, S. Matile. *Proc. Natl. Acad. Sci. USA* **100**, 11964 (2003).
28. G. Das, S. Matile. *Chem.—Eur. J.* **12**, 2936 (2006).
29. S. Matile, H. Tanaka, S. Litvinchuk. *Top. Curr. Chem.* **277**, 219 (2007).
30. J. J. Lavigne, E. V. Anslyn. *Angew. Chem., Int. Ed.* **40**, 3118 (2001).
31. A. Hennig, H. Bakirci, W. M. Nau. *Nat. Methods* **4**, 629 (2007).
32. J. Chandrashekar, M. A. Hoon, N. J. Ryba, C. S. Zuker. *Nature* **444**, 288 (2006).
33. S. Litvinchuk, N. Sordé, S. Matile. *J. Am. Chem. Soc.* **127**, 9316 (2005).
34. S. Litvinchuk, H. Tanaka, T. Miyatake, D. Pasini, T. Tanaka, G. Bollot, J. Mareda, S. Matile. *Nat. Mater*. **6**, 576 (2007).
35. L. J. Macpherson, A. E. Dubin, M. J. Evans, F. Marr, P. G. Schultz, B. F. Cravatt, A. Patapoutian. *Nature* **445**, 541 (2007).
36. L. Vial, P. Dumy. *J. Am. Chem. Soc.* **129**, 4884 (2007).
37. H. Tanaka, S. Litvinchuk, D.-H. Tran, G. Bollot, J. Mareda, N. Sakai, S. Matile. *J. Am. Chem. Soc*. **128**, 16000 (2006).
38. H. Tanaka, G. Bollot, J. Mareda, S. Litvinchuk, D.-H. Tran, N. Sakai, S. Matile. *Org. Biomol. Chem.* **5**, 1369 (2007).
39. S. M. Butterfield, M. L. Waters. *J. Am. Chem. Soc.* **125**, 9580 (2003).
40. S. Bhosale, A. L. Sisson, P. Talukdar, A. Fürstenberg, N. Banerji, E. Vauthey, G. Bollot, J. Mareda, C. Röger, F. Würthner, N. Sakai, S. Matile. *Science* **313**, 84 (2006).
41. S. Bhosale, A. L. Sisson, N. Sakai, S. Matile. *Org. Biomol. Chem.* **4**, 3031 (2006).
42. S. Bhosale, S. Matile. *Chirality* **18**, 849 (2006).
43. C. Thalacker, C. Röger, F. Würthner. *J. Org. Chem.* **71**, 8098 (2006).
44. A. Blaszczyk, M. Fischer, C. von Hänisch, M. Mayor. *Helv. Chim. Acta* **89**, 1986 (2006).
45. P. Talukdar, G. Bollot, J. Mareda, N. Sakai, S. Matile. *J. Am. Chem. Soc.* **127**, 6528 (2005).
46. P. Talukdar, G. Bollot, J. Mareda, N. Sakai, S. Matile. *Chem.—Eur. J*. **11**, 6525 (2005).
47. T. M. Fyles. *Chem. Soc. Rev.* **36**, 335 (2007).
48. A. P. Davis, D. N. Sheppard, B. D. Smith. *Chem. Soc. Rev.* **36**, 348 (2007).

49. J. T. Davis, G. P. Spada. *Chem. Soc. Rev.* **36**, 296 (2007).
50. R. S. Hector, M. S. Gin. *Supramol. Chem.* **17**, 129 (2005).
51. U. Koert, L. Al-Momani, J. R. Pfeifer. *Synthesis* **8**, 1129 (2004).
52. S. Matile, A. Som, N. Sordé. *Tetrahedron* **60**, 6405 (2004).
53. G. W. Gokel, A. Mukhopadhyay. *Chem. Soc. Rev.* **30**, 274 (2001).
54. P. Scrimin, P. Tecilla. *Curr. Opin. Chem. Biol.* **3**, 730 (1999).
55. Y. Kobuke, K. Ueda, M. Sokabe. *J. Am. Chem. Soc.* **114**, 7618 (1992).
56. J.-H. Fuhrhop, U. Liman, V. Koesling. *J. Am. Chem. Soc.* **110**, 6840 (1988).
57. T. Miyatake, M. Nishihara, S. Matile. *J. Am. Chem. Soc.* **128**, 12420 (2006).